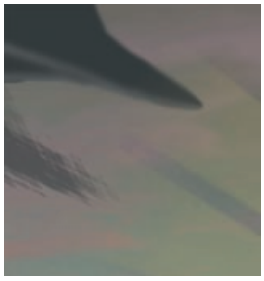

Coherent Data Collection Efforts in Support of Phalanx

Russell Rzemien and Jay F. Roulette

The Applied Physics Laboratory, in its role as Technical Direction Agent for the Phalanx close-in weapon system radar, designed and operates a coherent data collector to analyze radar system performance. This article presents examples of how coherent data analysis has helped program development efforts and provided insights into the performance of the Phalanx search radar. The topics discussed include radar system dynamic range, subclutter visibility, aircraft characteristics, surface target detectability, electromagnetic interference investigations, and radar environmental studies.
(Keywords: Clutter, Coherent, Phalanx, Radar.)

INTRODUCTION

Naval combatant ships, such as cruisers, destroyers, and frigates, have several weapon systems for defense against attacking aircraft and missiles. One of these systems is the Phalanx close-in weapon system (CIWS), which uses a short-range surveillance radar, a tracking radar, and a 20-mm gun to engage threats that penetrate the outer layers of defense (e.g., the ship-to-air missiles used to engage threats farther out from the ship). Because of its close-in defense role, little time is available for Phalanx to detect and engage attackers. Phalanx must cope with large levels of close-in sea clutter as well as strong radar returns from land and rain. The challenge for the radar designer is maintaining high sensitivity for detection of small, fast-moving targets while keeping the false alarm rate from clutter low.

Radar systems typically employ coherent signal processing techniques to meet these challenges.[1] Briefly, a coherent radar uses phase information of the echo as a discriminant to detect the presence of moving targets. Clutter echoes from land, sea, or rain tend to have relatively constant phase, whereas echoes from moving targets have phase shifts from the Doppler effect. Coherent signal processing techniques detect weak target echoes in the presence of clutter echoes orders of magnitude stronger; however, such processing works only if sufficient waveform stability is built into the radar.

The main demand on the system designer is to ensure that adequate stability and appropriate signal processing are available to perform the required detection task. The designer, when estimating radar performance, often uses simplified target and clutter models. Clutter and target characteristics are described statistically, since the radar reflections fluctuate in a manner too complex to be treated by exact mathematical methods. The power of aircraft echoes, for example, can fluctuate more than a hundredfold when the aircraft is changing aspect angle with respect to the radar

by only a few degrees. Clutter returns, particularly from land, are equally difficult to predict. Consequently, performance predictions are estimates that sometimes fall short when the environment deviates significantly from the model. Additionally, the models selected may not apply to the system under design. Such factors as radar band, waveform, polarization, antenna height, and sidelobes all have to be taken into account. Finally, the very nature of the land may be different from that assumed in the model. Simply describing a model as representing "land clutter" is too general. The radar returns from mountainous coastal clutter, for example, are far greater than the returns from desert beaches.

Acting in its advisory role to the Navy, APL employs a coherent data collection and analysis methodology as part of system performance assessment. Coherent digital radar data are collected from the system at a point before any signal processing. (Typically, the coherent data are collected from an in-phase digitized video channel, the I channel, and a quadrature digitized video channel, the Q channel. For the first version of the Phalanx coherent data collector [CDC], the coherent data were obtained from the radar in analog form and digitized by the collector.) Collecting the data before any processing provides the actual radar view of the environment and gives the analyst a powerful tool for assessing system performance in the real world. Because the input data rates to the signal processor easily exceed the capabilities of commercially available storage devices, APL built and operates a specialized recording device. The following section briefly describes the collectors built by the Laboratory. Subsequent sections describe how these devices have contributed to the Phalanx program development efforts.

PHALANX COHERENT DATA COLLECTORS

In 1980, the USS *Coral Sea* (CV 43) received the first CIWS afloat. This version, designated Block 0, had analog coherent processors for both search and track radars. At about the same time, an upgraded system was proposed to meet new threats. Designated Block 1 and first deployed aboard the USS *Wisconsin* (BB 64) in 1988, its purpose was to increase search surveillance volume coverage, provide the ability to acquire and engage faster targets, increase fire rate, and allow a larger magazine. As part of the upgrade, a new digital search radar processor and new search waveforms were proposed.

To support evaluation of this new radar, APL proposed constructing a coherent data collector. This device interfaced to both the Block 0 and Block 1 systems. For Block 0 data collections, the interface to the radar used the same synchronous detection circuitry and analog-to-digital (A/D) converters that were used in the Block 1 search processor. A digital interface was used for the Block 1 radar because it allowed collection of the identical unprocessed digital data used in the search processor. Regardless of the interface, search input (or burst) data rates were approximately 15 MB/s (12-bit A/D converters were used, one for the I channel and one for the Q channel, with a conversion rate of 5 MHz). Because the Block 0 systems were being phased out of the Fleet, most of the collection, analysis, and evaluation efforts went into the Block 1 systems.

Two collectors were built. The first was used for almost a decade.[2] Initially it interfaced with preproduction versions of the Block 1 radar, beginning with land-based testing at the Naval Air Warfare Center (NAWC), China Lake, CA. When designed in 1984, this collector used state-of-the-art streaming tape drives (145 KB/s sustained storage rate to a 9-track magnetic tape capable of holding approximately 40 MB of data), a modest hard disk array (1.1 MB/s sustained storage rate with a capacity of approximately 100 MB), and an embedded microprocessor-based system controller (see Fig. 1; also, for an overview of CDC architecture, see Rzemien, this issue). The speed of the various components limited the collection sector to approximately one-fourteenth of the total surveillance volume, and collection could be sustained for only 90 s. This limitation provided a "snap-shot" capability for radar environment studies and collections involving high-speed inbound targets.

The second collector (Fig. 2), built in 1993, made it possible to expand the collection sector to more than half the surveillance volume, thereby providing a more global picture of the radar environment. This collector has significantly greater storage capacity, which allows sustained collections for more than half an hour with a minimum-sized collection sector. The new parallel disk array can store data at a sustained rate of 8 MB/s and has a capacity of approximately 2.5 GB. The new tape drive unit can store data at a sustained rate of approximately 0.5 MB/s and can hold approximately 5 GB of date on a single tape cartridge. This capability proved to be invaluable in tests involving surface targets and electromagnetic interference. Surface target tests usually last longer than other types of tests, requiring longer collection times. Electromagnetic interference tests may also require long collection periods, although it is the uncertainty of the location of the interference (no *a priori* knowledge of where to set the collection sector) that makes maximizing the collection sector important. Likewise, studies involving collections of data on the radar's environment benefit from larger collection sectors.

A number of data reduction and analysis tools were developed to process the collected data. Data products range from simple amplitude histograms (useful for identifying problems in the A/D converters, among other things, or for determining the noise level at the

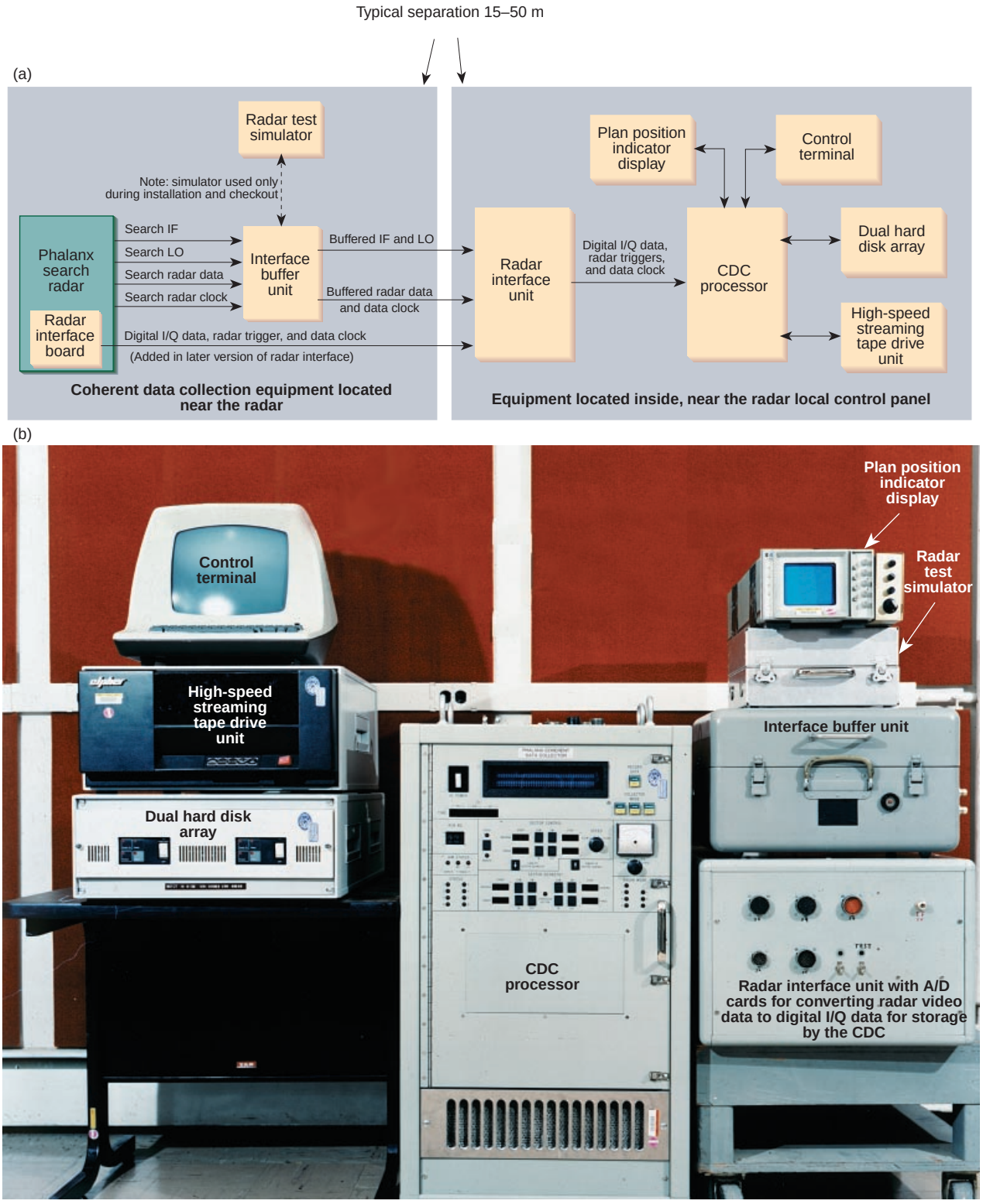

Figure 1. The first Phalanx CDC. (a) Conceptual block diagram. The buffered IF and LO signals, which are analog, were later replaced by the digital I/Q data signals that were sent directly from the Phalanx search radar to the radar interface unit. (IF = intermediate frequency [radar coherent received signal]; I/Q = in-phase/quadrature radar video signals; LO = local oscillator [reference signal used in radar interface unit to create I/Q videos].) The interface buffer unit is an all-weather piece of equipment because it is mounted alongside the Phalanx radar electronics enclosure, which is typically above decks, exposed to fog, rain, and sea spray. The remaining equipment is usually located close to the Phalanx local control panel, typically within 30 m of the radar. (b) Photograph of the first CDC, supporting peripherals, and test equipment. The many buttons and display windows in the center of the CDC processor were used to control the size and position of the collection sector. (A/D = analog to digital.)

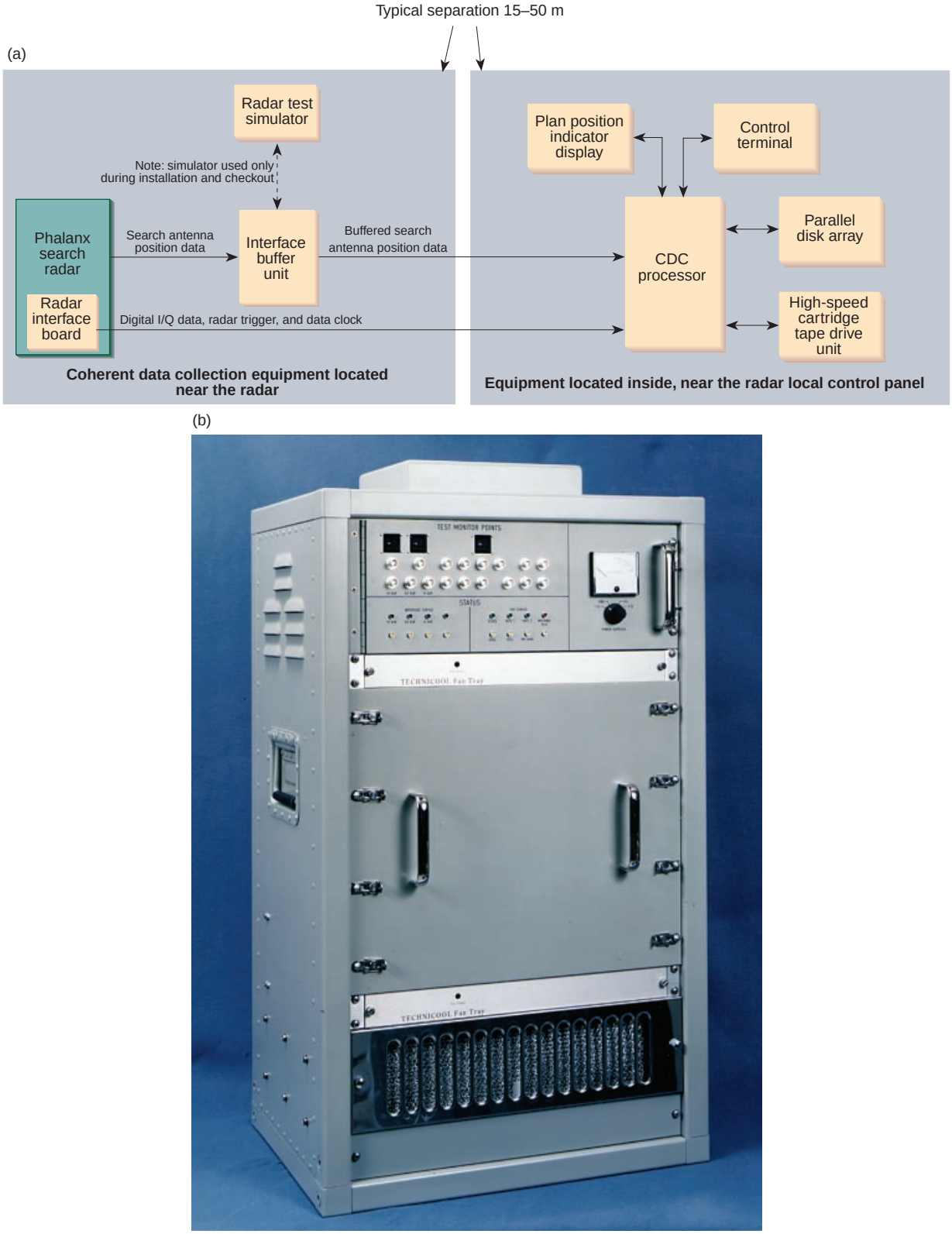

Figure 2. Upgraded Phalanx CDC installation. (a) Conceptual block diagram. The analog buffered IF and LO signals are no longer used; the digital I/Q data signals are sent directly from the search radar to the CDC processor. The interface buffer unit is used solely to send search antenna position information to the CDC processor. The radar interface unit is no longer used. (b) Photograph of the upgraded CDC processor. Its enclosure is the same size as that of the first collector, but the electronics are more sophisticated. The front panel contains test points and status lights only. Control is provided by a control terminal.

converter) to complex detection algorithms that simulate various radar signal detection processes. Examples of several such tools are provided in the following sections. The processing currently is performed on Sun Systems Sparc workstations, whose portability allows them to be taken into the field along with the collection instrumentation.

SYSTEM PERFORMANCE STUDIES

The first CDC was installed on the Ex-USS *Stoddard*, a target ship used by the Navy to support at-sea testing of systems. Testing occurred off the coast of southern California, with the collector interfacing to production support models (i.e., preproduction versions) of Phalanx. This testing provided the opportunity to observe system performance in the presence of land and sea clutter. The collected coherent data demonstrated the shortcomings of the then-existing land-clutter model and helped to establish the fundamental stability of the search radar.

Figure 3a is a range–azimuth plot showing the amplitude of clutter returns from an island off the coast of California. The island was about 3.6 km from the radar, corresponding to the closest range for land clutter under the old weapon specification. The model predicts that the average land mass radar cross section (wide-area mean) will not saturate the radar at this or farther ranges. Figure 3b, however, which is an amplitude histogram of these island data, shows that significant amounts of the returns are in saturation. The radar receiver noise is responsible for the Rayleigh distribution peaking at approximately 22 dB. If the receiver is not in saturation, the much larger land clutter should show a similar shape. However, the data are clustered at the saturation point of approximately 62 dB. (The saturation value is set by an intermediate frequency limiter, in the receiver gain chain, located just prior to the mixers that produce the I/Q video. This saturation level is set such that the input signals to the A/D converters will not exceed the maximum digital output value for the converter. In fact, some margin is left below this maximum value, since temperature and component aging can cause small changes in the overall system receiver gain.) Later studies (see data plotted in Fig. 7) confirmed that the model was at least an order of magnitude too low in predicting clutter returns.

A technique for evaluating the system stability provided important insights into the search receiver gain settings and system clutter cancellation capability. If search receiver gain is set too high, the system is more likely to go into saturation when clutter echoes are strong. In this nonlinear region, amplifiers do not respond to small signal variations to the same extent as when the system is out of saturation. Also, when the

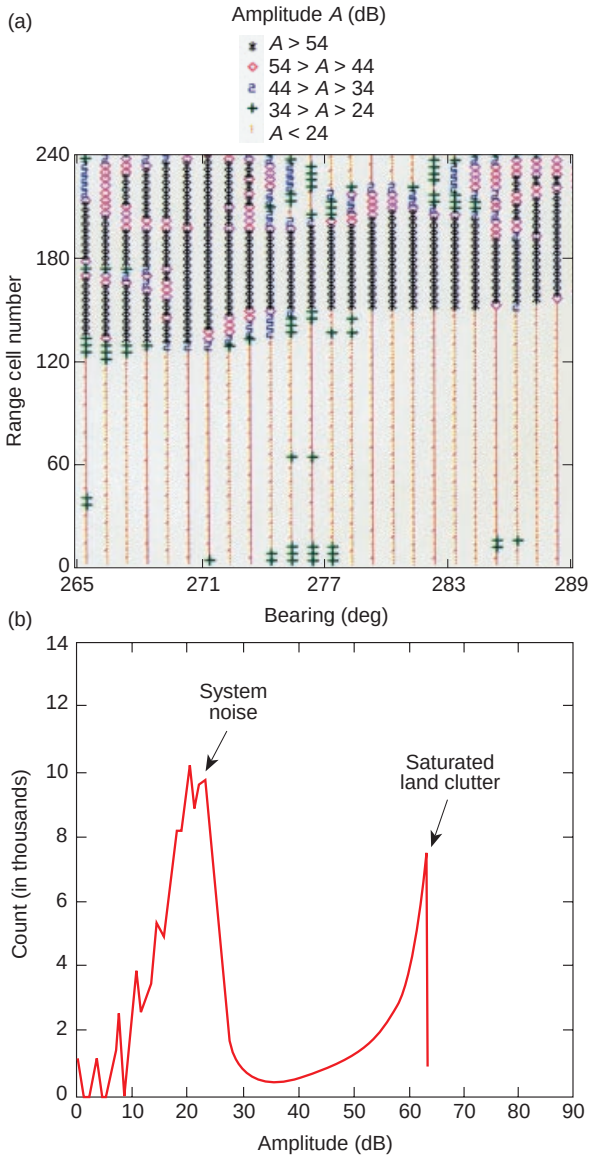

Figure 3. Land echo returns from an island about 3.6 km from the radar. (a) Range–azimuth plot of the returns, showing a large number of range cells exceeding 54 dB (data in black). Receiver saturation occurs at approximately 62 dB. Many of the cells shown in black are in saturation. (b) Amplitude histogram of the same radar returns. Note the large number of returns that reach the search receiver saturation level of approximately 62 dB.

amplifiers are in saturation, the thermal noise floor is reduced, as are the fluctuations normally used to detect targets. This phenomenon is referred to as small-signal suppression.

Figure 4 illustrates how the system stability is measured. Consecutive pulses of data are analyzed one range cell at a time. The pulses are processed using a fast Fourier transform (FFT) to determine the noise floor level of the middle filters, i.e., those filters not affected by the clutter. The end filters contain energy associated with clutter. The peak of the clutter is

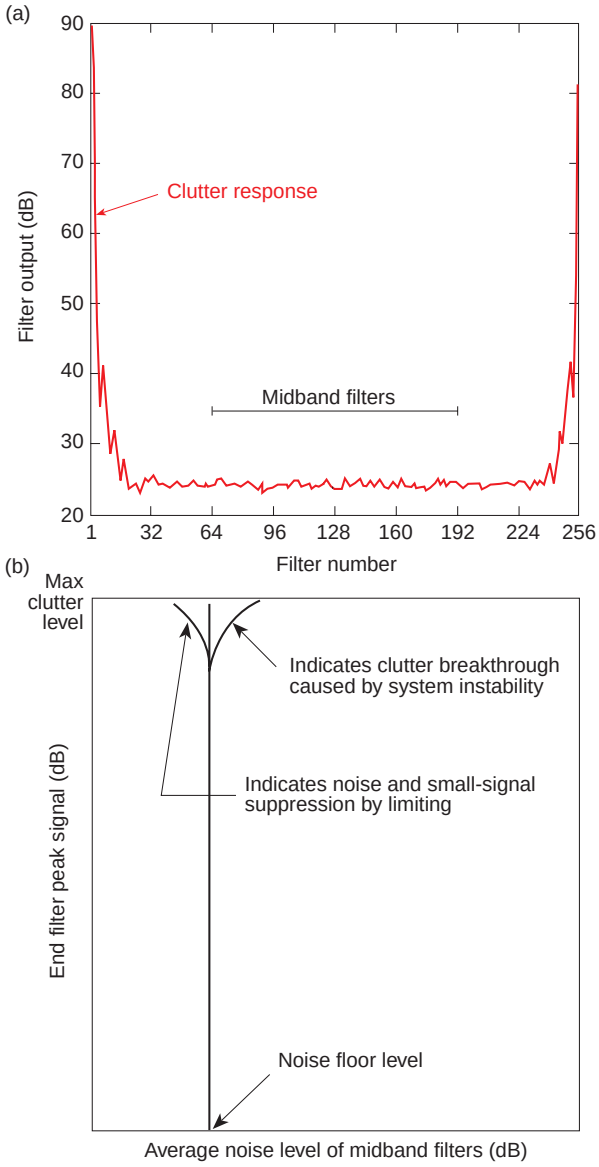

Figure 4. Dynamic range and system stability measurement. (a) Results of a fast Fourier transform at a fixed range. The stability measurement is made by comparing the noise level in the middle of the spectrum with the peak level in the end (clutter) filter, filter 1. (b) Three trends: noise suppression (line bends to the left), proper gain setting (line is vertical), and clutter breakthrough (line bends to the right). (Figure 5 shows the actual data.)

measured and associated with the average noise of the middle filters. These two values are used to plot a point on the system stability plot. The process is repeated at all range cells and for as large a bearing sector as is practical. Care must be taken to avoid fast-moving targets, since these can bias noise floor measurements.

A reasonable-size collection sector will contain a large range of clutter amplitudes and, usually, a number of noise-only range cells. (This is not always the case, particularly when the data are collected with the radar using a high pulse-repetition frequency waveform. For such a waveform, the clutter "folds" in, covering most, if not all, ranges and leaving few, if any, cells containing only system noise.) Ideally, the resulting stability plot should be a vertical line. Such a vertical stability plot means that the system noise is constant, as measured by the average of the midband filters, regardless of the input signal strength (see Fig. 4b). The noise level of these filters is significant, since targets must compete with this noise in the detection processing. In the case of small-signal suppression, the noise floor falls off as the input signal grows and drives the receiver into saturation. The plot in this case bends to the left (Fig. 5a). This does not result in greater detection sensitivity, since the target is likewise suppressed. In fact, the net effect is a reduction in target detectability because the signal-to-noise ratio generally is reduced.

A different phenomenon occurs when the receiver gain is set too low. In this case, noise associated with the transmitted signal (or the receiver local oscillator) will actually raise the receiver noise floor as measured by the midband filters. The level of the transmitted noise is usually several tens of decibels below the received signal level. However, if the signal is large enough, this noise may actually exceed the receiver noise. The raised noise floor reduces target detectability, since the target signal-to-noise ratio is reduced as the noise floor rises. This raised-noise phenomenon is called clutter breakthrough, and its presence indicates that the radar system stability is less than the dynamic range of the receiver. System stability provides a measure of the level of noise induced, either by the transmitter instabilities or by the receiver local oscillator, on an otherwise clean echo. One can think of this as low-level, broadband noise riding on the echo. The dynamic range of the receiver is the amplitude range of signals from the noise floor to saturation (i.e., the 1-dB compression point). As an example of how this works, consider a system with 40-dB stability (i.e., the "noise" associated with the transmitted pulse, system receiver, local oscillator stability, etc., is 40 dB below the echo) and a dynamic range of 50 dB. If the clutter echo is 20 dB below the receiver saturation point, the associated noise will be 10 dB below receiver noise. The receiver noise is barely affected. If the echo is 10 dB below saturation, the associated noise will be equal to the receiver noise. The total system noise is now 3 dB larger than the receiver noise alone. Finally, if the received echo is just at the saturation point, the total system noise will be slightly more than 10 dB higher than receiver noise alone. In terms of the stability plot, this effect is seen as a bending of the line to the right as the maximum signal level increases (Fig. 5b).

A properly tuned system exhibits neither of these effects. With optimal tuning, the effects of small-signal

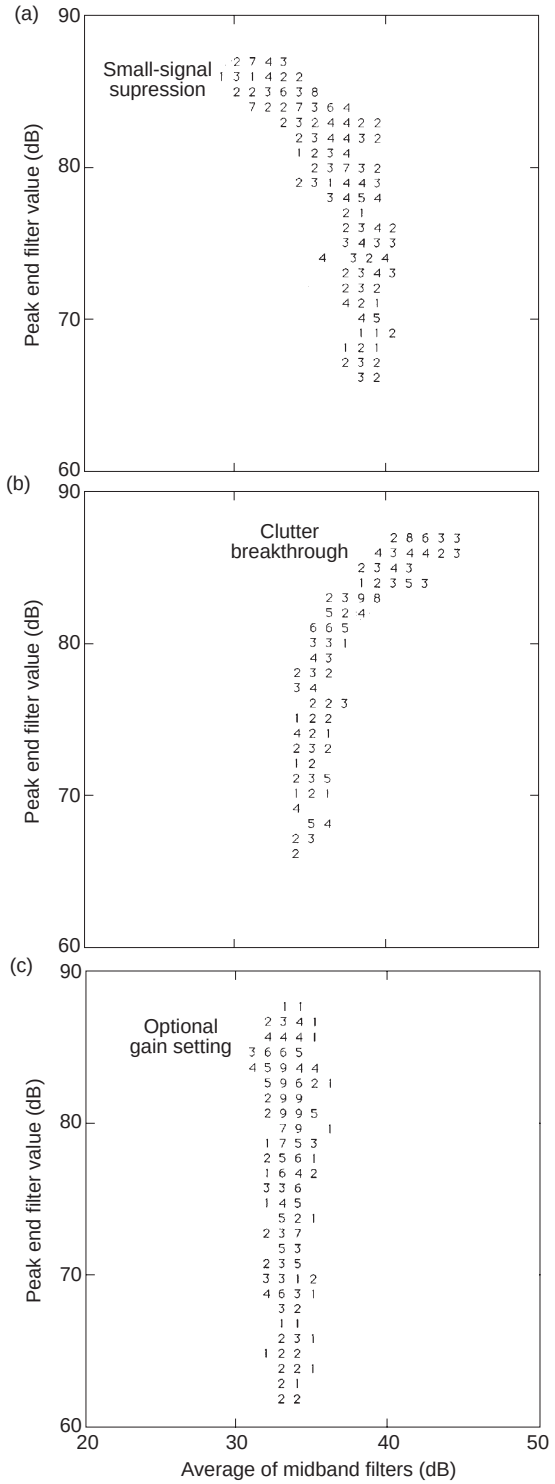

Figure 5. System stability measurements of the Phalanx radar for various settings of the receiver gain chain. Vertical axes show the value of the end (clutter) filter. Horizontal axes show the average value of approximately half the filters, centered on the midband filters. This presentation prevents clutter, which spreads outside the end filter, from corrupting the floor estimate. (a) The effects of small-signal suppression when the level of the clutter return forces the receiver into saturation, suppressing the system noise. (b) Breakthrough of transmitted noise. (c) Correctly adjusted gain chain, where the suppressed radar noise is balanced by the transmitted noise reflected from the clutter.

suppression are offset by the rising level of clutter breakthrough. The net result is the vertical line shown in Fig. 5c. Without infinite-dynamic-range receivers and perfectly stable systems, this is the best that can be achieved. One final point concerning Fig. 5: the stability plots can display the results of each calculation as a number starting with 1 for the first occurrence of a particular pair of noise floor and peak amplitude; if the same pair recurs, the plotted value is incremented from 1 to 2. In Fig. 5 the value reaches a maximum at 9. The statistical nature of the noise floor is responsible for the spreading of the "line." On an alternative plot, the average value for a given peak can be taken and only this point plotted, thereby approaching the line shown in Fig. 4b.

The method just described was used to evaluate the Phalanx search receiver. At the time of the testing, the radar manufacturer was evaluating different versions of the synchronous detection circuitry. This circuitry is used to convert the receiver intermediate frequency signal to the in-phase and quadrature videos that are digitized by A/D converters. Depending on the receiver configuration, both small-signal suppression and clutter breakthrough were observed. The results of the APL analysis aided the radar manufacturer in selecting the final configuration for the production version of the synchronous detector and in setting the receiver gain structure for optimal performance.

CLUTTER MODEL VERIFICATION

Phalanx, like many radar systems, performs best in a benign environment. As indicated in the introduction, modeling system performance using the statistical behavior of targets and the environment can lead to erroneous performance predictions. One of the most significant uses of the collected data was comparing the models used when estimating system performance with the clutter environment actually seen by the radar. In the case of clutter, the coherency of the data was of less significance than the availability of large dynamic range amplitude data.

Inputs to most sea- and land-clutter models can include one or more of the following: radar band or frequency, antenna polarization, grazing angle of the incident beam, and terrain or sea-state characteristics. The models usually provide a measure of the backscattered energy in the direction of the radar by specifying a normalized radar cross section for the clutter. This measurement allows the amount of energy scattered back at the radar to be determined from a few simple radar parameters, such as azimuth beamwidth and transmitted pulse range extent. A simple calculation then provides the analyst with the effective radar cross section of the clutter. Example comparisons of clutter

model predictions with environments actually seen by the radar are given in the following paragraphs.

The sea-clutter model first used by the Phalanx program predicted the level of clutter as a function of sea state and the incident grazing angle of the radar beam on the sea surface. Sea state, as an indicator of surface roughness, is an estimate at best. Tables exist that relate sea state to such observables as wind velocity, wave height (measured from crest to trough of the largest one-third of all the waves), and required fetch (the distance a given wind has been blowing over open water).[3] The instrumentation for measuring these parameters, however, is almost never available to personnel involved in routine data collection exercises. One can look at the predicted range of clutter returns and compare it to clutter data collected over various conditions. In doing so, two conclusions can be reached. First, finding clutter echoes that exceed the model by several decibels is not difficult. Second, a phenomenon known as sea spikes is not at all accounted for in the model. Sea spikes have larger cross sections than the background distributed sea clutter, reach values on the order of 1 to 10 m^2, and persist for several seconds. They may be associated with breaking waves that are forming whitecaps, resulting in large echoes that can generate false detections.

Figure 6 shows clutter measured using CDC data and predictions from both the original Phalanx weapons specification sea-clutter model and a newer model developed in light of the original model's shortcomings. It is apparent that the newer model predictions are a better match to the observed data. At small grazing angles, the measured data suggest that the clutter falls off more rapidly than either model predicts. This discrepancy may result from the difficulty of obtaining a good measure of the normalized clutter cross section; at those angles, the echo amplitudes approach the level of the receiver noise floor, which makes accurately estimating clutter echoes very difficult. Fortunately, this region is not of great significance, from a systems engineering perspective, since the clutter level is too small to affect the system's detection sensitivity. The dip in the data below the model predictions at large grazing angles results from the saturation of the receiver by the in-close sea clutter.

The deficiencies of the old model were apparent during at-sea testing, where the sea-clutter environment generated more false alarms in the radar processor than originally expected. As a result, the more robust sea-clutter model is now used for performance predictions. Model modifications include an increase in the average backscatter predictions, incorporation of the spectral spread associated with the backscatter (previously it was assumed that the clutter had no Doppler spread), and incorporation of sea spikes into the model.

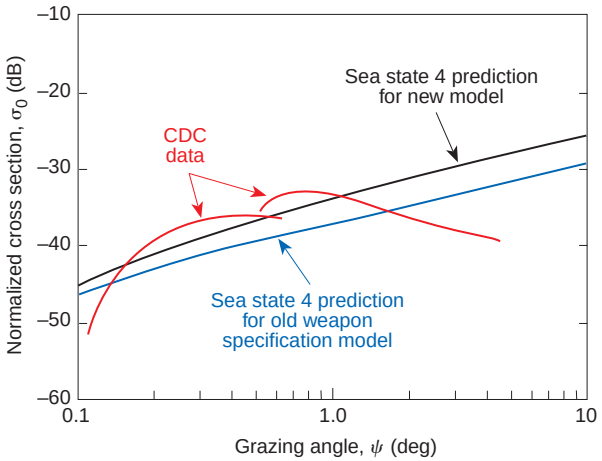

Figure 6. Comparison of measured sea clutter with the original Phalanx weapon specification sea-clutter model predictions. The old weapons specification sea-clutter model underestimated the strength of sea-clutter returns. The newer model does a better job of estimating sea-clutter echoes. Grazing angle refers to the incident angle of the radar signal as measured from the sea surface. Thus, smaller grazing angles imply farther ranges from the radar. The fall-off of the CDC data at grazing angles less than 0.15° can be explained by the fact that the amplitude of the clutter echo is close to the level of the receiver noise, making it difficult to accurately estimate the strength of the sea clutter. The lower-than-expected cross section estimates for grazing angles greater than 1° are caused by the effects of receiver saturation on the amplitude of the close-in sea clutter; that is, instead of the clutter amplitude continuing to rise at closer ranges, it stays fixed because of the receiver's saturation limit.

The land-clutter model likewise underestimated the magnitude of the land backscatter. From a qualitative point of view, this is perhaps best seen from the model prediction that land masses beyond about 32 km would produce clutter echoes weaker than radar system noise (i.e., the echoes would not be "seen" by the radar). The effect of this prediction on radar performance was significant since search processing takes this range into account when determining the length of time needed before radar data should be processed for detections. (This is the concept of "fill pulses"—those pulses transmitted to fill the time until echoes from the farthest clutter are received. Coherent processing should not begin until these faraway pulses are being received; otherwise, the discontinuity caused by the late arrival of faraway clutter echoes in the processed pulse train can cause the filter to produce a signal of sufficient strength to generate a false alarm.)

Another prediction from the model was that the land echoes would not saturate the receiver; however, testing of the system at sea showed that many false alarms were generated when the radar was close to large land masses. In this case the saturation suppressed the noise floor, lowering the detection threshold. (The detection threshold is set on the basis of the measured value of the processor noise floor. If the floor drops

artificially low because of saturation, and the radar suddenly comes out of saturation, the threshold may not readjust quickly, and the system noise can be sufficient to generate detections, i.e., false alarms.) The data collection and analysis efforts described in the preceding section (System Performance Studies) showed the false alarms to be the result of dynamic range limitations in the receiver. System tests in the presence of large land masses provided the first indication of problems. The actual cause was not found, however, until the coherent data were collected and analyzed.

These clutter model verification efforts produced two results. First, the gain chain of the radar was optimally adjusted to balance receiver noise suppression against clutter breakthrough. The result is a constant noise floor regardless of the level of the clutter. This, in turn, keeps the false alarm rate under control. Second, the land-clutter model used in the Phalanx program was changed. Figure 7 is a plot of predicted clutter-to-noise ratio at the receiver A/D converter as a function of range from the radar. Predictions inside of 3.6 km are not given because system performance is not defined that close to land. The yellow line indicates the level of land-clutter returns based on the original Phalanx weapon specification model. The points are from land-clutter measurements. The large discrepancy between the model and land-clutter data led to the adoption of a new land-clutter model for the Phalanx program. The model, adapted from earlier APL efforts in support of the NATO antiair warfare program, provides a better fit to the data and greater fidelity in terms of the temporal, spatial, and Doppler statistics of the clutter.

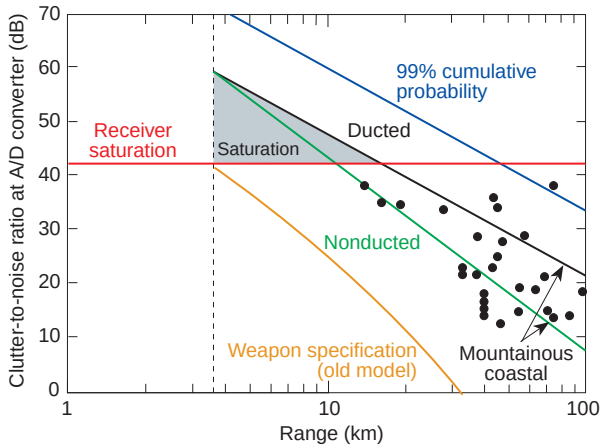

Figure 7. Predicted values (lines) and measured values (points) of land-clutter echoes. Note that the original weapons specification (yellow) predicted no land-clutter saturation (outside of about 3.6 km) and echo strength at or below system noise for land returns from farther than 32 km. Lines plotted with the new model (green, black, and blue), except for the 99% cumulative probability, are calculated using wide-area mean reflectivity.

AIRCRAFT DATA COLLECTIONS

Many different types of aircraft data have been collected using the CDC. In general, the Phalanx search radars easily detect fixed-wing jet aircraft. The types of scenarios usually flown against the radar are chosen to evaluate the tracking radar and to test for performance in multipath environments, in jamming situations, and against multiple attacking targets. From the search radar perspective, these targets are not particularly challenging. Data have been collected for many different types of aircraft, usually with the intent of providing a record of system coherency during the test. Analysis of the data reveals a typical "skin" return for the target. That is, an FFT of the return signals shows a strong signal shifted from the clutter and located at a frequency corresponding to the Doppler shift caused by the reflections from the aircraft structure (fuselage and wings). Evidence of jet engine modulation is shown in Fig. 8. The target skin return is centered on filter 17 at range cell 40. The effects of the engine modulation can be seen in the raised filter levels on either side of the skin return. These levels are approximately 10 dB higher than the same filter outputs seen at different ranges. (See Fig. 8 caption for further details). The dwell time on target for the Phalanx search radar is not sufficient to resolve the individual jet engine modulation lines. To observe these lines, one would need either to use a slower scan rate across the target or to process the Phalanx track radar signals.

Of greater interest are cases involving electronic countermeasures. Figure 9 shows representative data taken when the aircraft is carrying a self-screening jammer. The raw amplitude data (Figs. 9a and 9b) show the effects of the barrage jammer; i.e., all range cells have large amplitudes representing the noise power of the jammer being received by the search radar. In such an environment, coherent processing was used to distinguish the target from the elevated noise floor created by the jammer. Figure 9c shows the target at range cell 212, clearly distinguishable from the noise background. This type of analysis is effective in determining the ability of the radar to detect aircraft in this jamming environment.

Additional analysis was performed to demonstrate the ability of the radar to determine aircraft elevation by comparing detection data across antenna tiers. In the test, CDC search data were processed to identify the location of an aircraft flying over the radar at a high elevation. The radar detection data were analyzed to determine the angular extent of the target, an indirect measure of the strength of the target return. The target was detected both in the horizon beam and in one of the elevated beams. By comparing the relative amplitudes of these detections, one can estimate the elevation of the target. This information can be used in threat evaluation.

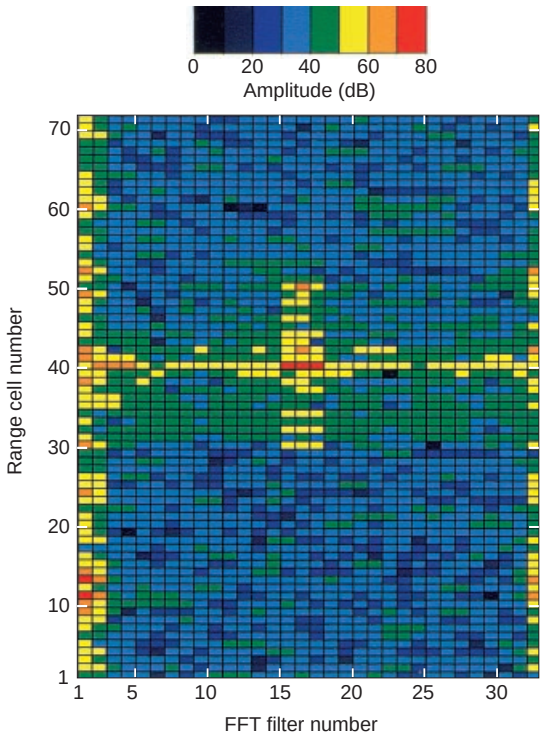

Figure 8. Fast Fourier transform of echoes from a jet aircraft. The aircraft is in range cell 40. Note the strong "skin" return in filters 16 through 18 and the smaller returns associated with jet engine modulation in the adjacent filter. Filter responses at range cells 1 through 29 and 51 through 72 should be compared. The elevated filter levels in range cells 30 through 39 and 41 through 50 are artifacts of pulse compression waveform processing. In this data set, the transmitted pulse was phase coded to allow an 11-to-1 pulse compression. Pulse compression involves coding the transmitted signal and then using this coded information to compress the range extent of the received signal. This technique improves range resolution while allowing the average energy on target to be as large as practical, given various system constraints such as transmitter duty cycle, transmit pulse repetition frequency, and antenna scan rate. Upon compression in the receiver, however, range "sidelobe" responses are produced that can be considerably larger than the receiver noise. In the case of Phalanx, the 11-to-1 compression ratio resulted in the range spreading shown.

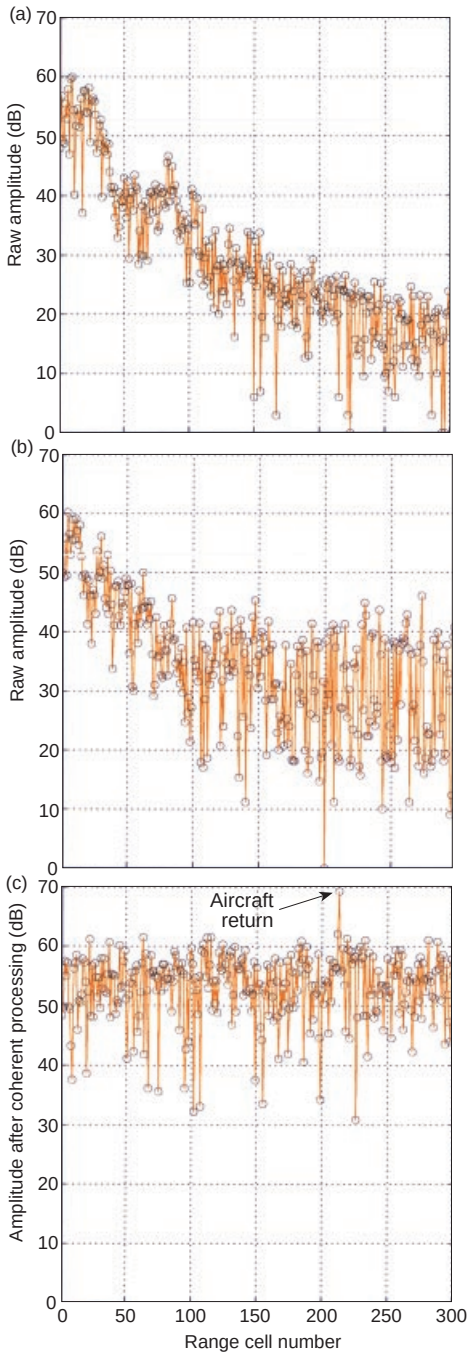

Figure 9. Representative data taken for aircraft carrying a self-screening jammer. (a) Raw amplitude range profile of region near where the aircraft carrying the self-screening jammer is flying. This plot shows the fall-off of sea clutter with range from the radar. There are about 35 range cells/km. By range cell 240 (about 7.2 km from the radar) the sea clutter has fallen to the level of system noise. (b) The barrage jammer is continuously transmitting noise in the band of the radar receiver. The noise makes identifying the range of the aircraft impossible without further processing of the echoes. The jammer has elevated the receiver noise floor by more than 15 dB. (c) After coherent processing of the data, the aircraft can be seen at range cell 212. The aircraft returns build up faster than the random noise pulses, making it possible for the aircraft returns to "grow" out of the noise. Processing consists of both pulse compression (discussed in caption of Fig. 8) and 32-point FFT filtering. This plot is a range profile for filter 25, the filter in which target response was maximum. Note that the filtering rejects the sea clutter, thus producing a relatively flat output response at all ranges.

Helicopters are a class of target of particular interest. As a threat to the ship, the helicopter can hover at a fixed distance from the ship with no relative velocity. The skin of the helicopter causes no Doppler shift to the echo and by itself would be rejected along with the clutter. A noncoherent processor, which depends on spatial movement of a target for detection and tracking, would probably reject such a target. However, the fast rotating blades of the helicopter modulate the radar signal, producing Doppler shifts. A coherent processor will detect this energy. Additional processing could then correlate the presence of this Doppler-shifted energy with the stationary source, and thereby identify the target as a helicopter.

Figure 10 shows the effects of blade modulation. The data collected were from a helicopter hovering a

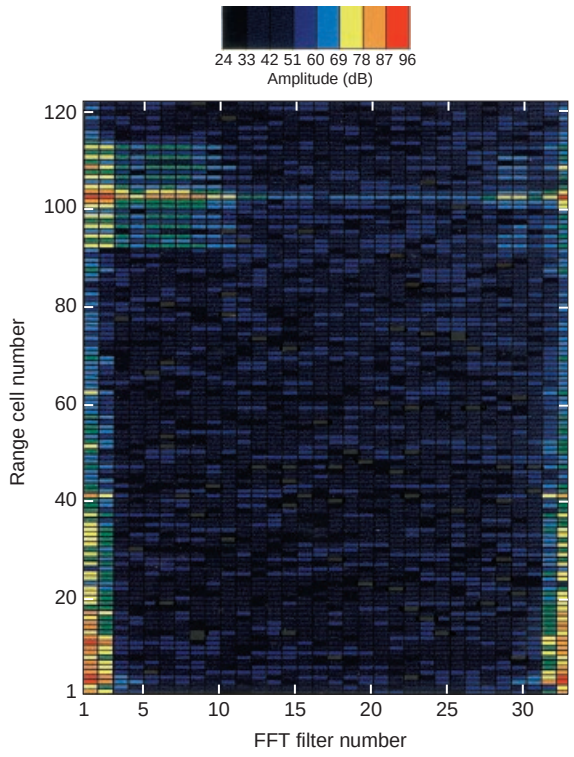

Figure 10. Fast Fourier transform of echoes from a helicopter. The helicopter is located at range cell 102, and the skin return is in filters 1, 2, 31, and 32. Compare these returns with the sea-clutter returns in the same filters at ranges 1 through approximately 40. A process that rejects the sea clutter will also reject the helicopter skin return. However, the helicopter also causes filter responses in the higher-velocity filters. These responses are due to the Doppler shifted echoes from the high-speed rotor blades. These echoes will pass through normal coherent clutter rejection processing, resulting in detections.

few kilometers from the radar. The skin return of the helicopter is readily apparent in the low-velocity Doppler bins (Filters 1, 2 and 31, 32 at range cell 102) of the FFT. Note the strong returns, caused by the rotating blades, spread across the Doppler filters. (The range spreading is due to pulse compression, as explained in Fig. 8). Although this energy is spread across the filters, radar processing would detect it even though the skin return is rejected along with other stationary clutter. (Compare the helicopter skin return to that of the sea clutter, which is particularly strong in the first 40 range cells.)

PHALANX SURFACE MODE

Operations in littoral waters increase the possibility of assault by small attack boats. These threats may pop out from behind commercial shipping or oil platforms and dash at combatants. The Navy is testing a forward-looking infrared (FLIR) camera on Phalanx that allows the weapon system's gun to be directed at such attackers. The FLIR camera is used to aim the gun accurately at the approaching threat, with firing initiated by the operator. APL supported tests involving both the search radar and the FLIR camera, which gave the Laboratory an opportunity to analyze radar performance against small surface craft.

Two types of surface craft were used in the testing. The first was a high-speed attack boat about 12 m long and capable of speeds up to 20 m/s. This boat is representative of threats one might encounter in regions such as the Arabian Gulf or the Adriatic Sea. The second craft was a small inflatable rubber boat about 4 m long and capable of speeds up to 8 m/s. This type of vessel could hold a couple of people and might be used for harassment or for firing guns or small rockets.

The boats were run in various patterns to simulate either direct inbound assaults at the ship, such as suicide missions, or parallel paths for harassment or sniping. The parallel path pattern results in little or no Doppler shift with respect to the ship, making target discrimination in clutter more challenging. Analysis of the data showed that target detection performance was adequate. However, issues concerning false-alarm rates were not completely addressed and would have to be considered if an automatic surface-tracking capability were to be added to Phalanx.

AT SEA WITH THE NAVY

Because the Phalanx CDC has been used primarily to support ongoing development work, most of the data collected came from installations at either land-based test sites (NAWC, China Lake, CA; the Naval Surface Warfare Center [NSWC], Port Hueneme, CA; NSWC, Dahlgren, VA) or else aboard test ships (the target ship, ex-USS *Stoddard*; the chartered commercial vessel, *Arctic Salvor*; and the *Self-Defense Test Ship*). In February 1995, the collector was installed aboard an active Navy ship deployed in the Arabian Gulf. The data were collected to assess Phalanx performance in the presence of strongly ducted land-clutter echoes.

Because Phalanx waveforms are highly range ambiguous, a modified waveform was used to obtain an unambiguous view of the environment. In this mode, the radar transmitted a narrow-range pulse approximately every 1.3 ms, making it possible to view clutter unambiguously for more than 170 km. (High-powered surveillance radars can see clutter at ranges considerably greater than this distance, although the relatively modest power of the Phalanx radar prevents it from seeing such long-range clutter except in the rarest circumstances.) Tests conducted about 30 km from a mountainous coastline did not indicate any apparent degradation of radar performance. However, very little ducting was observed.

The most interesting land-clutter data were obtained when the ship was entering the port of Fujairah, United Arab Emirates. This city is located on the Arabian Sea and has in its background rugged mountains that extend along the coast for many kilometers. Data could be collected at ranges much closer than the 30 km usually seen in the earlier tests. Data were collected at ranges up to 8 km from the coast and provided the first unambiguous look at the environment as seen by Phalanx. These data are valuable because Phalanx, which operates at a higher frequency than most surveillance radars, provides significant input for testing land-clutter modeling algorithms since radar frequency is known to affect the magnitude of the echo.

A Fleet Problem Resolved

The ship used during the Arabian Gulf tests has two Phalanx mounts installed midship, facing port and starboard. During the at-sea tests, the number of false detections rose significantly when both mounts were radiating. However, on one occasion the seas were very smooth, almost like glass, and under these conditions, no false alarms were seen. Data collected on this phenomenon were analyzed and revealed that the clutter returns were being modulated slightly by interference pulses from the other Phalanx mount. The amount of modulation, probably caused by nonlinear responses in the front-end electronics of the radar receiver, was enough to cause the coherent processor to output false detections (Fig. 11). Key to false-alarm generation was the synchronous nature of the interference. Interference pulses from one radar would line up in time at just the right intervals to produce significant outputs from the receiver processor. As a result of this analysis, APL proposed a minor change in the waveform pulse repetition intervals.[4] Although minor from an implementation point of view, the change unsynchronized the pulse repetition intervals between the two mounts without significantly affecting the detection performance of the search radar. Once unsynchronized, the interference pulses will not generate detections in the radar processor. The proposed modification has been successfully tested aboard other active Navy ships. After some additional tests the modification will be installed in the Fleet.

FUTURE EFFORTS

The Phalanx CDC will continue to support development efforts as needed. Several enhancements to the CDC are planned, assuming sufficient funding becomes available:

- The addition of an internal Global Positioning System recording capability. This information is

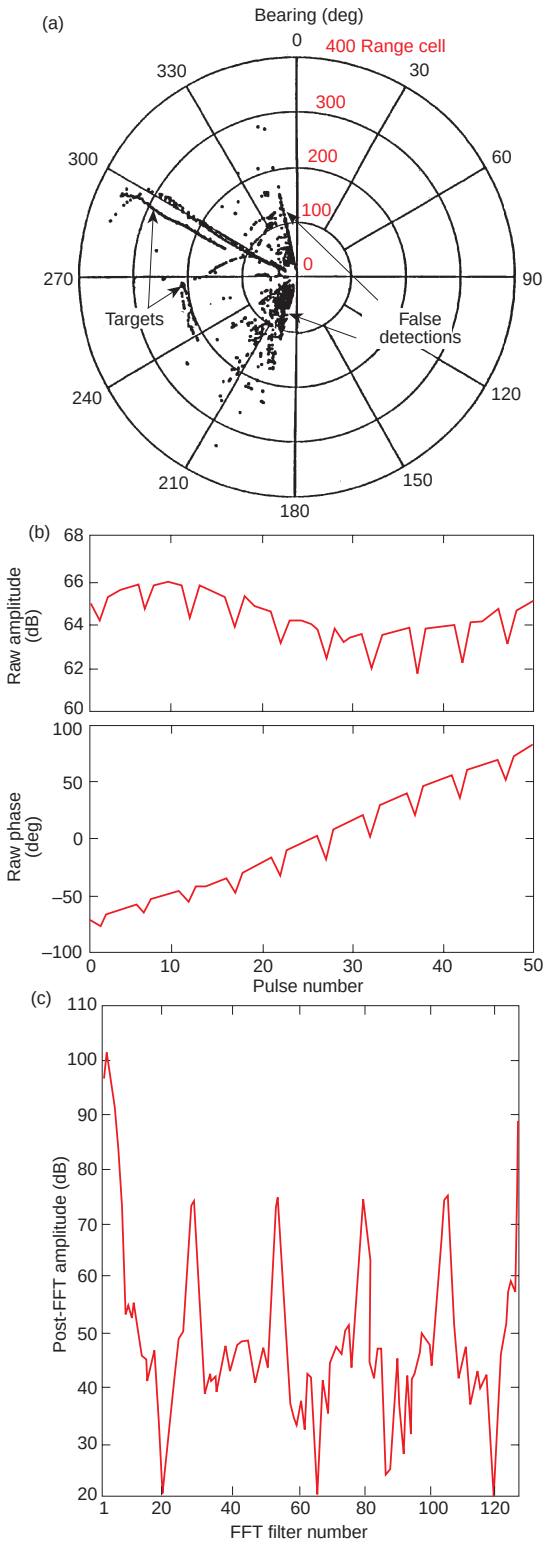

Figure 11. Phalanx mount-to-mount interference resulting in false detections in the presence of sea clutter. (a) A plan position indicator plot with targets and false detections. (b) Effect on the amplitude and phase of clutter returns (modulation) caused by the interference at a fixed range. Pulse number refers to consecutive samples, once per radar transmission, at that range. (c) Effect on a coherent process of the small amplitude and phase perturbations caused by the modulation. The figure shows the output of FFT filters operating on this type of data. The large peaks in the middle of the plot would cause detections in a coherent processor.

particularly valuable when collecting data associated with land-clutter studies.

- Internal processing of the collected data to provide a real-time display of the environment. This enhancement will allow test personnel to better direct data collection sectors and will extend the useful collection time for the system.
- Addition of a weapons control group processor port. Such a port will permit collection of search radar detection and track radar data directly into the CDC.

Recent testing aboard the *Self-Defense Test Ship* has demonstrated the capability for collector operation from a remote site. This capability will make it possible to collect data on missiles or other targets of interest that normally could not be collected, given that personnel must be removed from the ship during testing. In addition, modifications to the digital interface circuitry now make it possible to collect data from the radar without affecting the search radar signal processor. Previously, the interface card that was used to extract the radar coherent data was inserted in the slot normally occupied by part of the radar asynchronous pulse detection circuitry. Although this change normally did not affect performance significantly, it did result in a nonstandard configuration. The effect on the system was noticed only in cases where significant amounts of asynchronous interference were present. With the new circuitry, the radar regains this part of its processing. Thus, CDC can now be used during tests without affecting any aspect of radar performance.

Further analysis efforts are planned to investigate interesting phenomena observed during some of the tests described in preceding sections. For example, during the surface-mode testing it was noted that the amplitude of boat echoes behaved in a surprising manner (Fig. 12). As the antenna of a scanning radar passes over small targets (i.e., small with respect to the beamwidth of the antenna radiation pattern), one expects to see the signal strength of the target rise to some value and then fall off again as the beam passes by the target. The signal variation traces out the antenna gain pattern. Figure 12a shows this effect. Examination of the boat data, however, revealed a different pattern. In many cases, the pattern was modulated by a series of dips. The number and depth of the dips varied from scan to scan, and the dips were not seen on all scans. Although it is well known that target cross sections vary with time, the rapid rate of fluctuations was a surprise. The total time on the target for a single scan is less than 10 ms. As shown in Fig. 12b, the pattern varied several times in this interval. Normally, the sea state and the position of the target are assumed to be essentially frozen during these intervals. Naturally, some motion occurs; this motion is responsible for the phase shifts used for detecting the target. However, the mechanisms usually

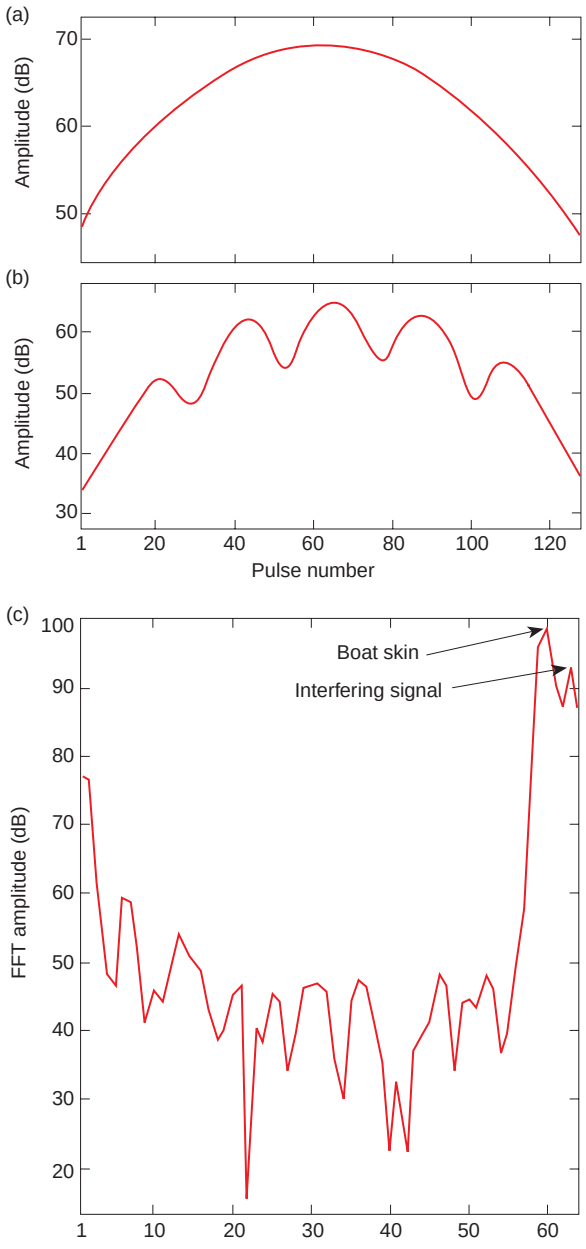

Figure 12. Surprising behavior of boat echoes during surface-mode testing. (a) Signal return showing normal amplitude variation as the antenna scans past the target. This is the expected two-way azimuth gain profile of the search antenna at the elevation of the target. (b) Scalloping pattern observed on inbound boat target, with dips and peaks that suggest an interfering signal at a slightly different Doppler frequency from that of the target. (c) Fast Fourier transform of a data set containing the scalloping pattern. The skin line is the larger peak in filter 60. The "interfering" signal, in both this plot and all others examined, is in a higher filter and at a lower amplitude. In Phalanx, the higher filter numbers (for unambiguous velocities) correspond to slower target velocities. Thus the interfering signal has a lower "velocity" than the target skin velocity.

invoked to explain the scalloped amplitude response—multipath fluctuations or changes in target aspect angle—do not have time to come into play.

The origins of this phenomenon remain unknown. The scalloping pattern suggests interference between two reflectors, offset in Doppler frequency but similar in amplitude, and an FFT of the data does indeed show two peaks (Fig. 12c). The larger peak, which also has the higher Doppler frequency, is probably the skin return from the boat since the range rate associated with the Doppler shift correlates well with velocity of the boat. The second peak is lower than the first in both amplitude and velocity, usually by several meters per second. Assuming the second peak is really caused by a second scatterer, the question remains: What is its origin? Several sources have been suggested, none wholly satisfactory. The "rooster tail," or spray kicked high into the air by the boat, might have both the required cross section and reduced Doppler frequency, but the smaller inflatable boat displays this effect without having a noticeable rooster tail. Another possible source is the multipath image of the boat. The problem here is that no mechanism has been proposed to explain the relatively large decrease of the "image's" Doppler relative to the boat. Other candidates include wake phenomena associated with the boat or other reflectors present on the boat itself. The data have not been exhaustively studied, however, and further analysis should lead to an explanation.

Another interesting phenomenon was observed during the at-sea tests in the Arabian Gulf. During the first days of the test, large numbers of false alarms were seen in the upper beams of the radar. The weather was partly cloudy with some small showers in the area, but the detections were not apparently associated with rain. There was some obscuring of visibility, and sand was reported to be blowing in the air. There is a symbiotic relationship between the interference and the sea clutter, and it is possible that a similar phenomenon is occurring between the interference and the rain clutter or sand clutter in the atmosphere. Coherent data were collected and will be examined to see what can be learned about this phenomenon.

CONCLUSIONS

As the preceding examples show, coherent data collection and analysis are effective tools, not only in analyzing Phalanx search radar system performance, but also in identifying and solving system performance problems. The effects of the problems may be readily observable (such as the false alarms associated with electromagnetic interference, or false detections generated in the presence of saturating clutter), but the fundamental mechanisms causing these problems (synchronous interference or improper gain settings in the receiver) are not readily apparent. In cases such as the scalloping patterns observed in the boat data or the high-angle false alarms, further analysis may lead to an understanding of these phenomena and consequently to a more fundamental understanding of both the radar and its interaction with the environment.

REFERENCES

[1] Nathanson, F. E., Reilly, J. P., and Cohen, M. N., *Radar Design Principles*, 2nd Ed., McGraw-Hill, Inc., New York, pp. 1–41 (1990).
[2] Rzemien, R., "Coherent Radar—Opportunities and Demands," *Johns Hopkins APL Tech. Dig.* **17**(4), 386–400 (1996).
[3] Blake, L. V., *Radar Range–Performance Analysis*, Artech House, Inc., Norwood, MA, p. 307 (1986).
[4] Taylor, S. A., *Presentation of CIWS Intraship EMI Data,* JHU/APL F20-95U-099, The Johns Hopkins University Applied Physics Laboratory, Laurel, MD (1995).

ACKNOWLEDGMENTS: The authors thank the following individuals, who have contributed much toward making the Phalanx CDC effort a success: Paul R. Bade, Ronald J. Clevering, John P. Marple, Daryl I. Tewell, and Brian A. Williamson for development and systems work; Sidney A. Taylor for radar analysis; Alan H. Landay for data reduction development support; W. Charlene Eveland, Charles P. Richards, Charlotte R. Silva, and Ronald F. Wolff for technical and fabrication support; and John H. Baker and Thomas L. Vanskiver for in-house and, especially, field installation and operation support.

THE AUTHORS

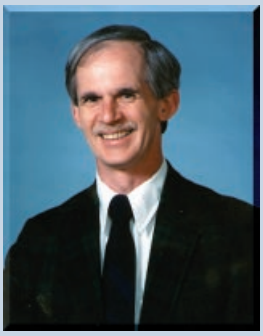

RUSSELL RZEMIEN is a Senior Professional Staff physicist in the Air Defense Systems Department's Combatant Integration Group. He earned a B.S. degree in physics from the University of Rhode Island in 1975 and an M.S. degree in physics from the University of Colorado in 1979. Since joining APL in 1979, he has specialized in digital signal processing and instrumentation of radar systems. He is co-holder of a patent for a coherent radar digital data collector and sampling technique for noncoherent transmitter radars. He served as lead hardware design engineer for the Laser Radar, MK 92, Phalanx, and Tartar Coherent Data Collectors, and he was lead engineer for the Radar Intermediate Frequency Experimentation Facility. Other projects include the Pacific Missile Test Center Digital Data Collector, AN/SPS-48C Detection Data Converter, and MK 92 Radar Processor. His e-mail address is Russell.Rzemien@jhuapl.edu.

JAY F. ROULETTE is a Senior Professional Staff engineer in the Air Defense Systems Department's Combatant Integration Group. He earned a B.S. degree in electrical engineering from Virginia Polytechnic Institute and State University in 1983 and an M.S. degree in electrical engineering from The Johns Hopkins University in 1988. Since joining APL in 1983, he has specialized in coherent data collection and analysis for various radars including the Phalanx, MK 92 MOD 6 and MOD 2, AN/SPS-48E, MK 23 TAS, and AN/APQ-164. Other projects include signal processing development for the TAS Adjunct Processor, systems engineering on a proposed high-frequency radar, systems engineering on proposed stepped-frequency waveforms, investigation of algorithms for interference rejection, and development of coherent waveforms for use in range-extended clutter. His e-mail address is Jay.Roulette@jhuapl.edu.